Soil Heat Transducers and Water Vapor Flow

J. W. CARY

Soil Heat Transducers and Water Vapor Flow[1]

J. W. Cary[2]

ABSTRACT

The heat flow through a silt loam, silty clay, and loamy sand were measured in a calorimeter at 7 and 36°C under matrix potentials near −0.3 bars. The transient thermal conductivity probe, the heat flux transducer, and deVries's theoretical method all gave low values of the apparent thermal conductivity at 36°C. An empirical correction was proposed for deVries's method that improved its agreement with the observed conductivities. The thermal vapor diffusion coefficients for the three soils were then calculated from his equation and compared with experimental values from the calorimeter. It was also shown that the thermal water vapor flow can be estimated if one knows the soil's saturated thermal conductivity, quartz content, water content, bulk density and temperature distribution.

Additional Index Words: thermal conductivity, thermal soil water flow, vapor diffusion coefficients, coupled heat and water flow, phenomenological coefficients.

WATER VAPOR diffusion across an air space between two moist, parallel surfaces, may be described by Fick's law as:

$$J_v = -D\nabla\rho_v \qquad [1]$$

where the symbols are defined in appendix A. If the vapor pressure gradient in the air space is fixed solely by the temperatures of the two surfaces, Eq. [1] may be expressed over the range of 0 to 45°C as:

$$J_v = -\beta\,(aT^2 + b)\,\nabla T \qquad [2]$$

where $\beta = 1$ (Cary 1966). When the space between the parallel surfaces contains soil, the value of β will depend on the properties of the soil. If J_v can be measured at two different temperatures under a fixed thermal gradient, β follows from Eq. [2] as

$$\beta = \frac{\triangle J_v}{a\triangle\,(T^2)}\,(\nabla T)^{-1} \qquad [3]$$

assuming β is independent of temperature. The parameter β may also be estimated from measurements of total heat flux made under a fixed thermal gradient at two different temperatures. The heat flux at a given temperature is

$$J_q = -\lambda\nabla T \qquad [4]$$

where λ includes the latent heat component carried by the vapor transfer. The temperature dependence of λ is largely due to the increased latent heat flow as

vapor flux increases with increasing temperatures. Consequently,

$$\beta \simeq \frac{\triangle\lambda}{H_v\,a\,\triangle\,(T^2)} \qquad [5]$$

when $\triangle J_q = H_v\,\triangle J_v$, $\beta \neq f\,(T)$, and ∇T is constant.

Methods for accurately observing J_v are tedious and require some experimental finesse. It is not surprising that only a few such measurements are available. Consequently, the purpose of the work reported here, was to measure λ at two different soil temperatures with a glass heat-flux plate and transient thermal conductivity probe to see if either method would lead to acceptable values of β through Eq. [5].

EXPERIMENTAL PROCEDURE

The net steady-state heat and water fluxes due to various thermal gradients were measured in the calorimeter sketched in Fig. 1. The calorimeter was mounted in an air-tight cylinder with only the flow tube outside. The whole system was housed in a constant temperature room. The heat loss from the calorimeter was measured as a function of the steady-state temperature difference between the warm and cool chambers. The heat loss calibration was done in two ways. First, the soil chamber was filled with water, the temperature of the cool chamber was held constant, and known amounts of heat were added to the warm chamber by adjusting the dc voltage across the heating coil. The heat flow across the water in the soil chamber was known from the thermal conductivity of water and the temperatures at the upper and lower boundaries of the chamber. This heat flux was subtracted from the rate of heat added to the warm water chamber. The difference was taken as the calorimeter heat loss expressed as mcal sec⁻¹ cm⁻² of porous plate area and plotted against the temperature difference between the warm and cool water chambers, as shown in Fig. 2. In the second calibration, the soil chamber was filled with air-dried loamy sand after sealing the porous plates off with thin discs to prevent wetting of the soil. The thermal conductivity of the loamy sand was measured in place with the conductivity probe. The calorimeter's heat loss then followed from this value as it did when water was in the soil chamber.
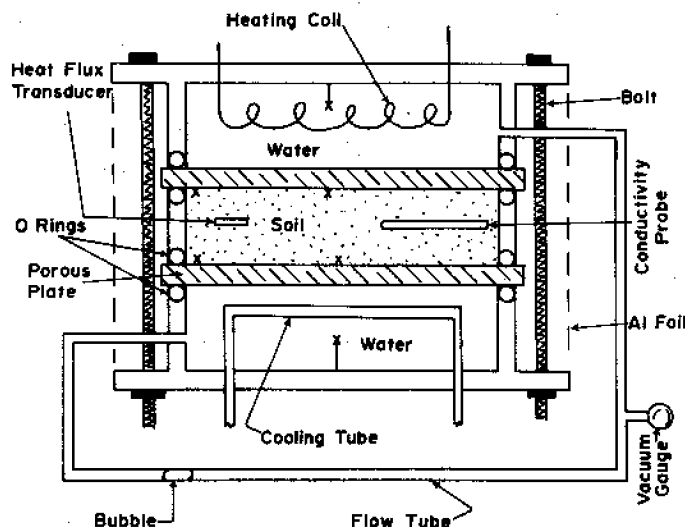

Fig. 1—A cross section diagram of the calorimeter used to measure soil heat flux. The crosses show the location of thermocouples. The soil chamber and the upper and lower water chambers were each 18.8 cm in diam and 5-cm high.
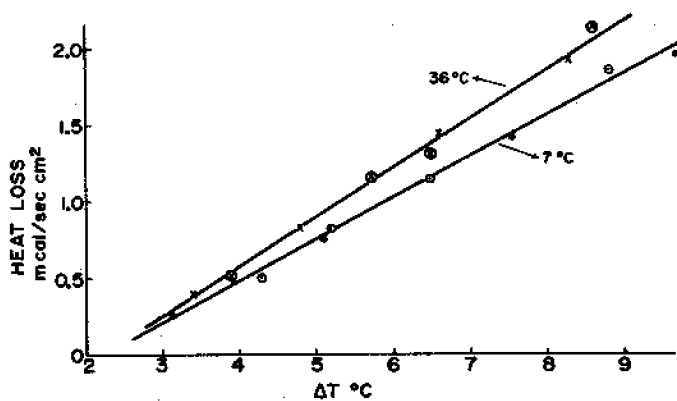
Fig. 2—Heat loss curves for the calorimeter. The crosses were measured at 36°C and the solid points of 7°C. The circled data points indicate the dry loamy sand in the soil chambers, while the uncircled points are for water.

The conductivity probe in the soil chamber was made from copper tube, 10-cm long with a 5 mm o.d. The heating wire was embedded in plaster inside the tube. The temperature of the tube's surface was measured with two thermocouples soldered to the outside and connected in parallel to a commercial thermistor compensated readout device. The energy input was 16.75 mcal sec^{-1} cm^{-1}, which gave a temperature rise of < 3°C over the 200-sec heating interval. Values of λ were calculated from the temperature rise data, using a slope fitted by least squares and the relation given by Jackson and Taylor (1965).

The heat-flux transducer was made from a piece of glass (0.2 by 2 by 3.5 cm) wrapped with a copper-constantan thermopile and coated with silicone rubber made for insulating electronic components. The transducer was 3.5-mm thick with a thermal conductivity < 1 mcal sec^{-1} cm^{-1} °K^{-1}. Its calibration constant was measured in the dry loamy sand during tests of the calorimeter's heat loss. The transducer's output during the calibration with water showed some scatter (±10%) when compared to the calorimeter's overall heat flow, indicating there may have been a bit of convection around the transducer under these conditions.

Three soils with the physical parameters listed in Table 1 were studied. Each soil was air-dried and poured through a stopper hole in the lucite ring that formed the side of the soil chamber in the calorimeter. The soil was then wet from the porous plates, which had a hydraulic conductivity of 5 × 10^{-3} mm hour^{-1} (cm H$_2$O/cm)$^{-1}$. This allowed reasonably uniform packing and good contact with the porous plates. The calibrations and soil measurements were each done at two temperatures. In one case, the water pumped through the cooling tube held the water in the bottom chamber at 4°C, while the air around the container holding the calorimeter was kept at 7°C. In the second case, these temperatures were 33 and 36°C, respectively. The net steady-state water flux from the warm to cool side of the soil was known from the movement of an air bubble in a horizontal glass tube as the water returned to the warm chamber.

At least 3 days were allowed for the soil water to equilibrate when the temperature was changed from 7 to 36°C or from 36 to 7°C. Fifteen hours was generally sufficient time for the soil to reach steady state following a change in thermal gradient.

RESULTS AND DISCUSSION

The measured thermal-conductivities are shown in Table 1, which also includes values calculated by the methods of deVries (1963). His method was calibrated for each soil (Kimball et al., 1976). The equation

$$\lambda = \frac{\lambda_w x_w + \lambda_s x_s k_s + \lambda_a x_a k_a}{x_w + x_s k_s + x_a k_a} \qquad [6]$$

was used in the form applied by deVries (1963) to Healy clay. A value for λ_s was obtained from

Table 1—Measured and calculated soil thermal conductivities for three soils at two temperatures with various thermal gradients in the calorimeter.

	∇T	λ Calorimeter	λ Transducer	λ Probe	λ DeVries
	°C cm^{-1}	mcal sec^{-1} cm^{-1} °K^{-1}			
Silt loam					
Avg. temp. 7°C	0.28	2.29	1.59		
$x_w = 0.337$	0.48	2.19	1.38		
$\varrho_B = 1.35$	0.20	2.20	1.79		
$\tau = -0.32$	0.53	2.47	1.55		
	0.31	2.03	1.68	1.91	
	0.37	2.38	1.67	1.89	
Mean		2.26	1.60	1.90	2.20
Avg. temp. 36°C	0.33	3.37	1.76		
	0.50	3.00	1.70		
	0.20	3.20	1.62	2.00	
	0.27	3.41	1.72	2.07	
Mean		3.25	1.70	2.04	2.40
Loamy sand					
Avg. temp. 7°C	0.46	2.22	1.35		
$x_w = 0.1$	0.30	2.43	1.40	2.05	
$\varrho_B = 1.5$	0.21	2.30	1.40	2.15	
$\tau = -0.3$					
Mean		2.32	1.38	2.10	2.30
Avg. temp. 36°C	0.26	3.85	1.68		
	0.36	3.61	1.68		
	0.40	4.06	1.73	2.35	
	0.19	3.71	1.67	2.29	
Mean		3.81	1.69	2.32	3.08
Silty clay					
Avg. temp. 7°C	0.42	1.93	1.16		
$x_w = 0.38$	0.52	1.98	1.14		
$\varrho_B = 1.2$	0.26	1.77	1.17	1.74	
$\tau = -0.3$	0.31	1.90	1.13	1.67	
Mean		1.90	1.15	1.75	1.90
Avg. temp. 36°C	0.30	3.13	1.44		
	0.38	2.87	1.43		
	0.22	3.05	1.54	1.86	
	0.52	2.50	1.44	1.89	
Mean		2.89	1.46	1.88	2.08

$$\lambda_s = 20 \frac{x_{qu}}{x_s} + 7 \frac{x_s - x_{qu}}{x_s} \qquad [7]$$

Equation [6] was first solved for k_s, using λ measured at 7°C and the water content of interest. The value of λ_a was taken from the curves given by deVries, which is also expressed by Eq. [2] in the form

$$\lambda_a = H_v (aT^2 + b) + \lambda_{air}. \qquad [8]$$

Values of k_a were obtained from

$$k_a = 2/3 \ (1 + \frac{\lambda_a}{\lambda_w} g_a - g_a)^{-1} + 1/3 [1 + (\frac{\lambda_a}{\lambda_w} - 1)$$
$$(1 - 2g_a)]^{-1} \qquad [9]$$

where $g_a = 0.33 - 0.295 \ x_a \phi^{-1}$, (DeVries, 1963).

At 7°C, the values given by the transient thermal conductivity probe were reasonably close to those observed in the calorimeter as shown in Table 1. At 36°C, the probe's values were much less than those from the calorimeter, as were λ values measured by the transducer and those calculated from Eq. [6]. Evidently, neither the probe nor the transducer measured all of the increase in latent heat at 36°C. It is not surprising that the transducer behaved in this way, however, the probe should have sensed the increase. Possibly, as the probe's surface temperature increased,

Table 2—Values of β calculated from the data in Table 1 or from Fig. 3.

Soil	Calorimeter	Water flux increase	Probe	Transducer	DeVries
		β values			
Silt loam	2.93	2.36	0.41	0.44	0.63
Loamy sand	4.57	3.49	0.69	1.64	2.46
Silty clay	2.93	2.26	0.41	1.61	0.57

contact between it and the soil decreased as water moved away in both the vapor and liquid phases.

All of the λ values given by the transducer were low because its conductivity was too low. Unfortunately, the conductivity of the silicone rubber insulating coat, was only 0.35 mcal sec^{-1} cm^{-1} °K^{-1}. However, even when the calibration constant for the transducer was adjusted to give the same heat flux as the probe and calorimeter at 7°C, λ values were still too small at 36°C.

The low values of λ given by Eq. [6] at 36°C likely resulted from deVries's method underestimating the temperature dependence of k_a. Data from this study suggested the empirical correction,

$$\lambda_{ao} = \lambda_a \left(1 + 0.07\ T \sin \frac{x_a}{\phi} \Pi\right) \qquad [10]$$

where the argument is in radians, and λ_{ao} replaces λ_a in Eq. [6] and [9]. Equation [10] is probably not valid for temperatures much above 36°C.

In view of the range of values of λ given by the different methods, it is not surprising that there is some difference of opinion concerning vapor flux and thermal conductivites (Kimball et al., 1976, Hadas, 1977).

Table 2 shows values of β calculated from Eq. [5] and the mean thermal conductivities in Table 1. A small adjustment of $\triangle\lambda$ was first made for the increased conductivity of water at 36°C associated with the calorimeter data. The λ values from the transducer were also adjusted by using a calibration constant for each soil that brought the 7°C measurement up to those given by the other methods. The "water flux increase" values of β came from Eq. [3] and the curves in Fig. 3, assuming all of the increase in water flux as temperature increased from 7 to 36°C was in the vapor phase. The discrepancy between β values from the calorimeter and the water-flux measurements could be due to a systematic error in heat-flux measurements, or a thermal liquid flow with a negative temperature coefficient.

The liquid flow, shown in Fig. 3, is the difference between the observed net flow at 7°C and the vapor flow predicted by Eq. [2], using measured values of β. The liquid flow is several times greater than that predicted by Philip and deVries (1957), based on the effect of temperature on surface tension of pure water. This problem has also been noted by Jury and Miller (974). Obviously some phenomena are involved in thermal liquid phase flow in moist soil that we do not yet understand. Heat of transfer coefficients used to describe the thermal liquid flow in the irreversible thermodynamic approach were 0.1, 0.05, and 0.8 cal g^{-1} for the silt loam, silty clay, and loamy sand respectively. These resemble values reported for other soils (Nielsen et al., 1972, p. 109).
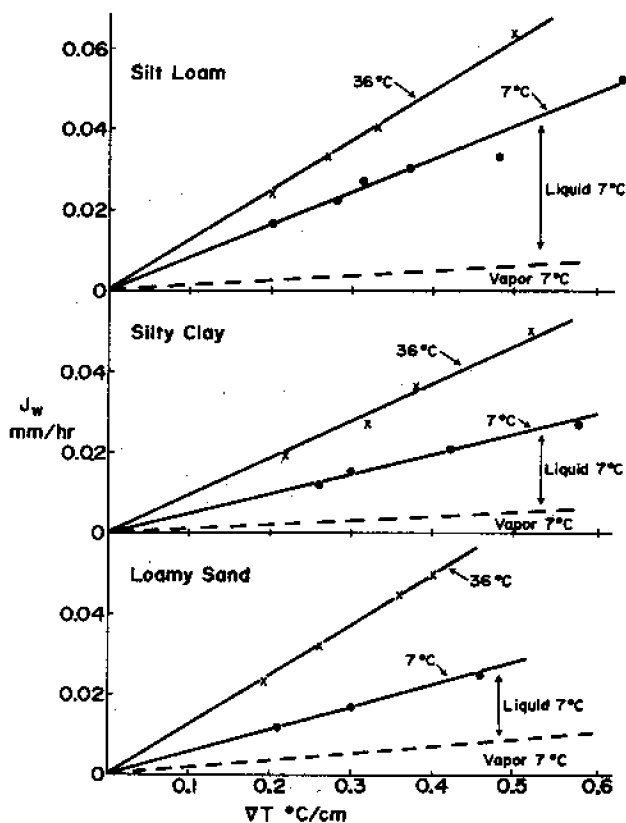

Fig. 3—Water flow caused by various soil thermal gradients. The crosses indicate net flow observed at 36°C while the solid points are net flow measured at 7°C. The dashed curve separates the vapor and liquid components of the net flux at 7°C.
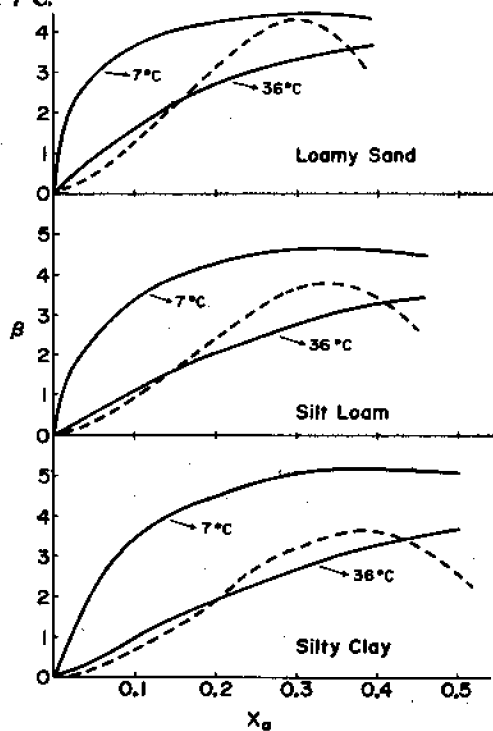

Fig. 4—The coefficient β as a function of the soil's volume fraction of air. The dashed lines are calculated from deVries's equation using the empirical correction, while the solid lines come from Eq. [17].
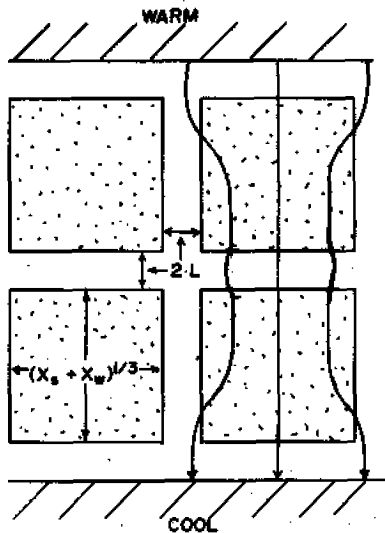
Fig. 5—A cross section schematic diagram of four soil aggregates separated by air space. The arrows suggest the major heat flow paths through the two aggregates on the right.

Values of β, based on the probe, the transducer, and Eq. [6], are too small. If, however, Eq. [10] is used in Eq. [6] and [9], reasonable values are obtained, as shown by the dashed lines in Fig. 4.

It is also possible to estimate β directly from a measurement of λ at saturation and some knowledge of the soil's physical properties. Suppose that the soil is made up of cube-shaped, saturated aggregates, surrounded by layers of air, as shown in Fig. 5. In this case:

$$[\,(x_s + x_w)^{1/3} + 2L\,]^3 = x_s + x_w + x_a = 1. \quad [11]$$

Thus:

$$2L = 1 - (1 - x_a)^{1/3}. \quad [12]$$

As suggested by the heat flow paths across the two aggregates on the right in Fig. 5, the heat passing through the aggregates will be about the same as the heat crossing the air spaces that lie in planes perpendicular to the heat flux. Consequently,

$$\lambda_a \frac{\varepsilon_a}{2L} \simeq \lambda_{agg} \frac{\varepsilon_{sw}}{(x_s + x_w)^{1/3}}, \quad [13]$$

and

$$\varepsilon_a + \varepsilon_{sw} = 1, \quad [14]$$

where "1" represents a "unit" temperature difference whose magnitude is fixed by the macroscopic soil thermal gradient. Equations [13] and [14] then give

$$\varepsilon_a = 2L\lambda_{agg} \,[\lambda_a (x_s + x_w)^{1/3} + 2L\lambda_{agg}]^{-1}. \quad [15]$$

Equation [8] provides values of λ_a and the thermal conductivity of the aggregates are approximately given by;

$$\lambda_{agg} = 20\, x_{qu} + 7\,(x_s - x_{qu}) + \lambda_w \gamma\, x_w \quad [16]$$

where γ, which is a water content matching factor, is obtained from Eq. [16], using a measured value of the saturated soil thermal conductivity for λ_{agg}.

The air spaces that lie in planes perpendicular to the direction of heat flux obviously experience larger thermal gradients than the soil as a whole. The numerical value of $\varepsilon_a (2L)^{-1}$ is the ratio of the thermal gradient across these air spaces to the overall soil thermal gradient. This is, of course, a major component of β. A factor is also needed to adjust the effective cross-sectional area through which most of the vapor diffuses. It is reasonable to suppose that this area will increase as the gas phase increases and the solid phase decreases. As a first approximation, then, one might expect:

$$\beta = \frac{\varepsilon_a}{2L} \frac{x_a}{x_s}. \quad [17]$$

The solid lines in Fig. 4 show β from Eq. [17] for the three soils studied here. The values are temperature-dependent as a direct result of the λ_a values used in Eq. [15]. The same type of temperature dependence was found by Jury and Letey (1979), when they calculated β values from an improved form of the Philip and deVries (1957) theory.

CONCLUSIONS

1) The heat flux plate, the transient thermal probe and deVries' (1963) theoretical method, all tend to give low values of the apparent thermal conductivity of warm, moist, unsaturated soils. deVries' method can be improved over the range of normal field soil temperatures with Eq. [10].

2) Thermal water vapor diffusion can be calculated from Eq. [2] for soils whose relative humidities are greater than 98% and whose temperatures are between 0 and 45°C. The coefficient β in Eq. [2] may be estimated from Eq. [5] and [6] using Eq. [10] for the apparent thermal conductivity of air. The parameter β may also be estimated from a measurement of the saturated soil thermal conductivity and Eq. [17].

3) It no longer appears that β is independent of temperature. Furthermore, the temperature dependence and even some of the mechanisms causing thermal liquid phase flow of soil water remain unknown.

APPENDIX A

Definition of Symbols

a	= constant = 1.56×10^{-5} mm hr^{-1} cm °C^{-2}
b	= constant = 2.72×10^{-5} mm hr^{-1} cm °C^{-1}
D	= water vapor diffusion coefficient in air, mm hr^{-1} cm^{3}g^{-1}
H_v	= constant associated with latent heat, taken as 16.3 mcal hour mm^{-1} sec^{-1} cm^{-3}
J_t	= heat flux, mcal sec^{-1} cm^{-2}
J_v	= vapor flux, mm hour^{-1}
k	= the ratio of the average temperature gradient in the granules and the corresponding quantity in the medium
L	= relative thickness of air film surrounding a soil aggregate
T	= temperature, °C
x	= volume fraction of a soil component
β	= dimensionless parameter describing the effect of soil properties on thermal water vapor transfer
Δ	= a difference
∇	= a gradient in one dimension of space
ε	= relative temperature difference
λ	= thermal conductivity, mcal sec^{-1} cm^{-1} °K^{-1}
λ_{agg}	= thermal conductivity of a saturated soil aggregate
λ_{air}	= thermal conductivity of air, not including latent heat transfer

ϕ = volume fraction of soil pore space
ρ_v = concentration of water vapor in air, g cm^{-3}
ρ_s = dry soil bulk density, g cm^{-3}
τ = soil water matrix potential, bars

Subscripts

a = gas phase
qu = quartz phase
s = solid phase
sw = combined solid and liquid phases
w = water phase

LITERATURE CITED

1. Cary, J. W. 1966. Soil moisture transport due to thermal gradients: Practical aspects. Soil Sci. Soc. Am. Proc. 30:428–433.

2. deVries, D. A. 1963. Thermal properties of soils, p. 210–235. *In* W. R. Van Wijk (ed.) Physics of plant environment. John Wiley & Sons, Inc., New York.

3. Hadas, A. 1977. Evaluation of theoretically predicted thermal conductivities of soils under field and laboratory conditions. Soil Sci. Soc. Am. J. 41:460–466.

4. Jackson, R. D., and S. A. Taylor. 1965. Heat transfer, *In* C. A. Black, (ed.) Methods of soil analysis, Agronomy 9: (Part 1) 345–360. Am. Soc. of Agron. Madison, Wisc.

5. Jury, W. A., and J. Letey. 1979. Water vapor movement in soil: Reconciliation of theory and experiment. 43:000–000 (this issue).

6. Jury, W. A., and E. E. Miller. 1974. Measurement of the transport coefficients for coupled flow of heat and moisture in medium sand. Soil Sci. Soc. Am. Proc. 38:551–557.

7. Kimball, B. A., R. D. Jackson, R. J. Regiato, F. S. Nakayama, and S. B. Idso. 1976. Comparison of field-measured and calculated soil-heat fluxes. Soil Sci. Soc. Am. J. 40:18–25.

8. Nielsen, D. R., R. D. Jackson, J. W. Cary, and D. D. Evans, (ed.). 1972. Soil water, Am. Soc. of Agron., Madison, Wis.

9. Philip, J. R., and D. A. deVries. 1957. Moisture movement in porous materials under temperature gradients. Trans. Am. Geophys. Union. 38:222–232.